Electronic Supplementary Information

The Hexagonal Perovskite $Ba_{0.5}Sr_{0.5}Co_{0.8}Fe_{0.2}O_{3-\delta}$ as Efficient Electrocatalyst for Oxygen Evolution Reaction

Lulu Tang,[a] Wanqun Zhang,[a] Dan Lin,[a] Yi Ren,[a] Hui Zheng,[a] Qinxin Luo,[a] Lianwei Wei,[a] Huimin Liu,[a] Junhua Chen,[b] and Kaibin Tang*[ac]

[a.] Department of Chemistry, University of Science and Technology of China, Hefei, 230026, China

[b.] Physics Department, School of Electric Science and Applied Physics, Hefei University of Technology, Hefei, 230009, China

[c.] Hefei National Laboratory for Physical Sciences at the Microscale, University of Science and Technology of China, Hefei, 230026, China

E-mail: kbtang@ustc.edu.cn

Calculation details:

The density functional theory (DFT) calculations were carried out with Cambridge Sequential Total Energy Package (CASTEP) code.[1] The generalized gradient approximation (GGA) method with the Perdew-Burke-Ernzerhof (PBE) functional was applied to the exchange-correlation potential. The ultrasoft pseudo-potentials (USP) were used for treating the core electrons and the energy cutoff was set as 400 eV for the plane wave. The self-consistent field (SCF) tolerance was 1×10^{-6} eV. A centered 6 × 6 × 1 k-points mesh were employed for surface calculation and the density of states (DOS) calculation. The PDOS band center was calculated using the equation: band center = $\frac{\int Ef(E)dE}{\int f(E)dE}$, where f(E) is the DOS value and E is the electron energy.[2]

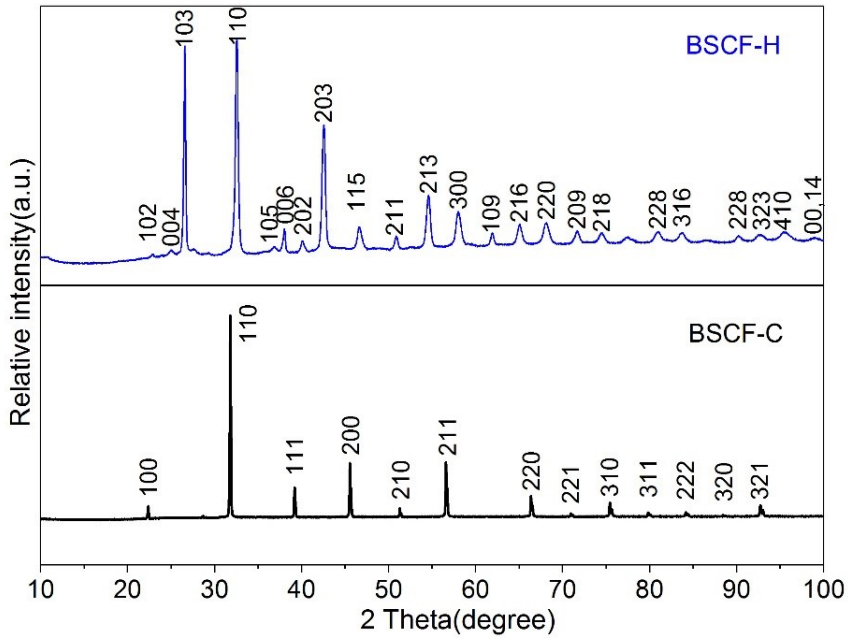

Fig. S1. XRD patterns of the as-prepared BSCF-H and BSCF-C powders.

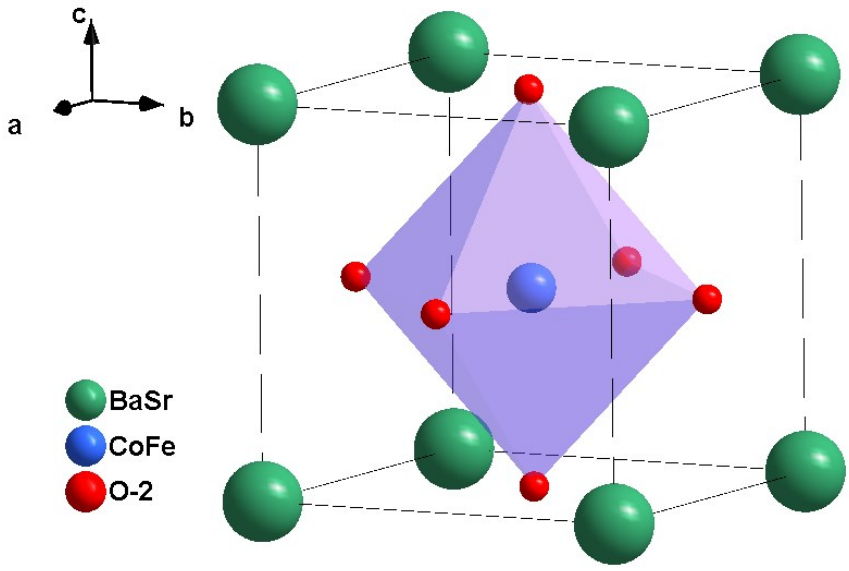

Fig. S2. Schematic presentation of the cubic BSCF-C crystal structure

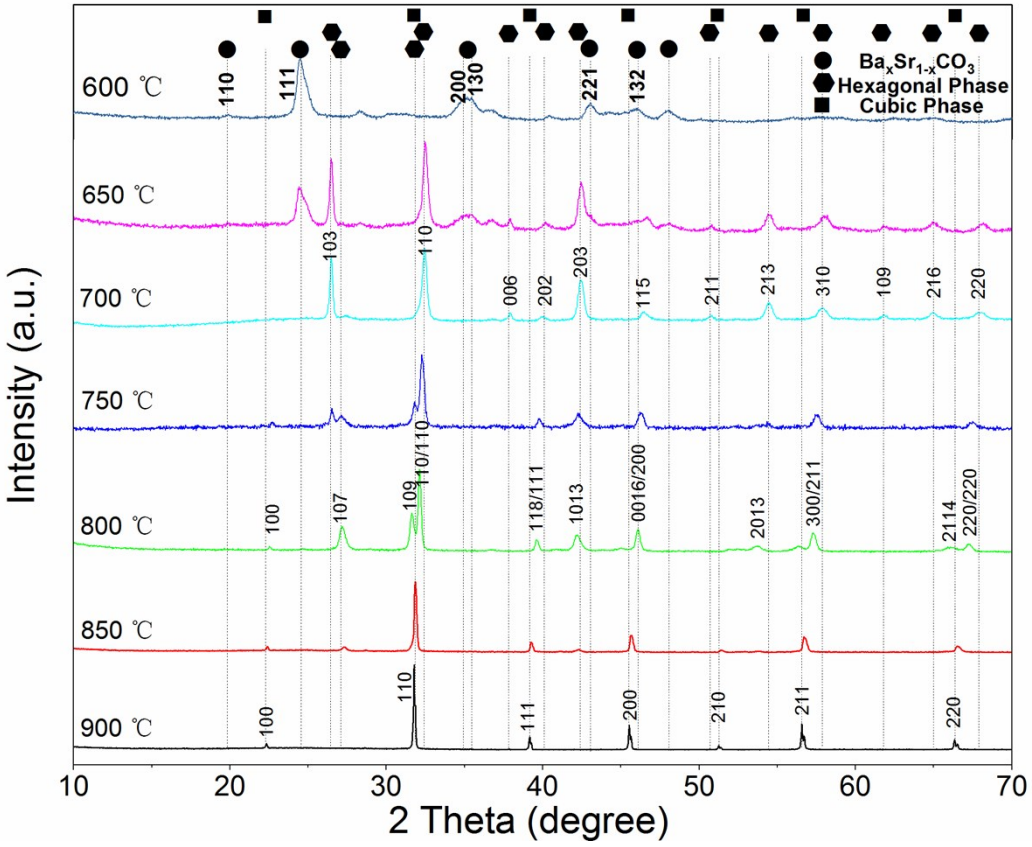

Fig. S3. XRD patterns of the powders obtained by the calcination of BSCF solid precursor for 10 h at various temperatures, 600 ℃, 650 ℃ ,700 ℃,750 ℃,800 ℃, 850 ℃ and 900 ℃, respectively.

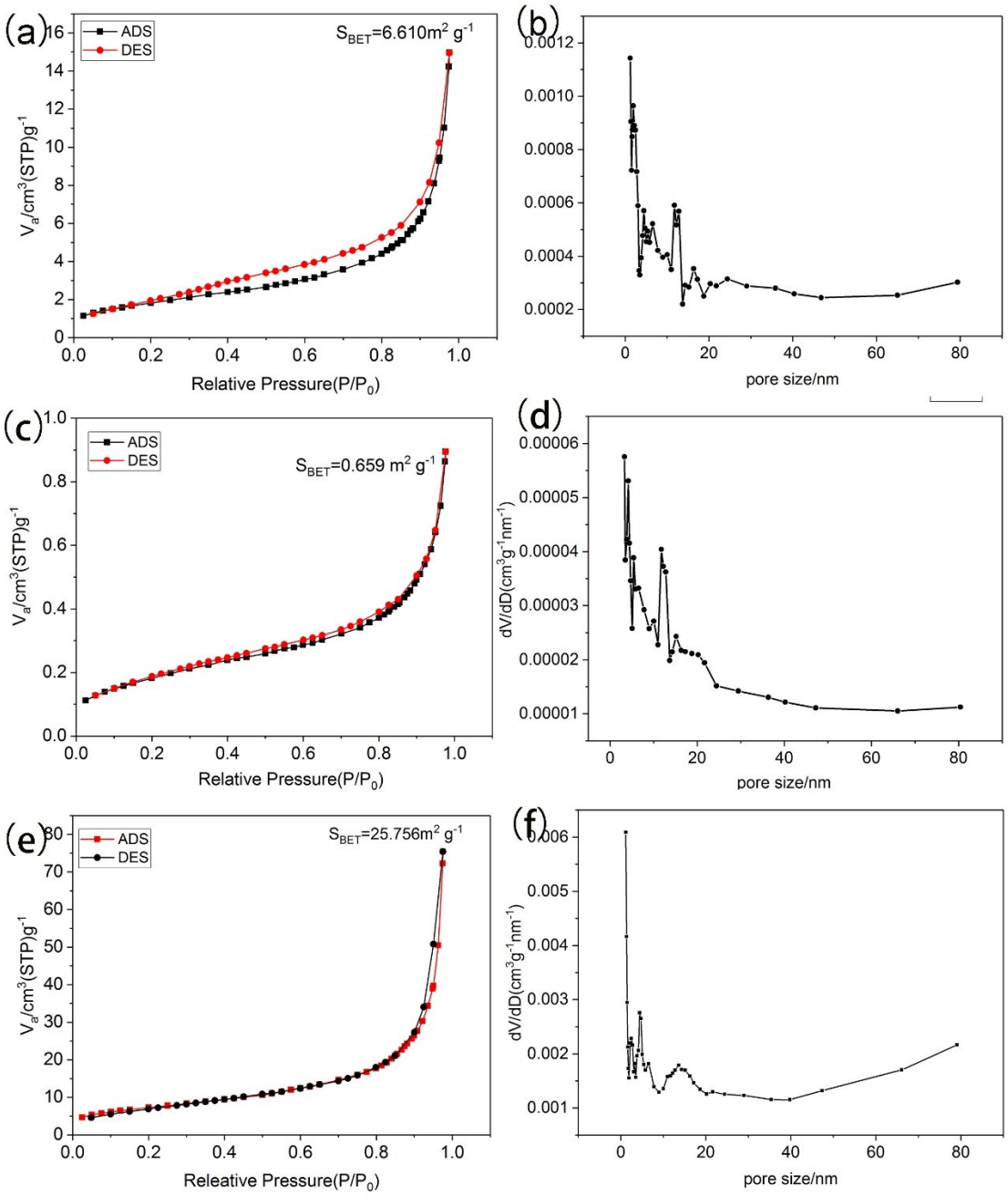

Fig. S4. (a) N_2 adsorption/desorption isotherm curves of BSCF-H, (b) BJH pore size distribution plots BSCF-H, (c) N_2 adsorption/desorption isotherm curves of BSCF-C, (d) BJH pore size distribution plots BSCF-C, (e) N_2 adsorption/desorption isotherm curves of RuO_2, (f) BJH pore size distribution plots RuO_2.

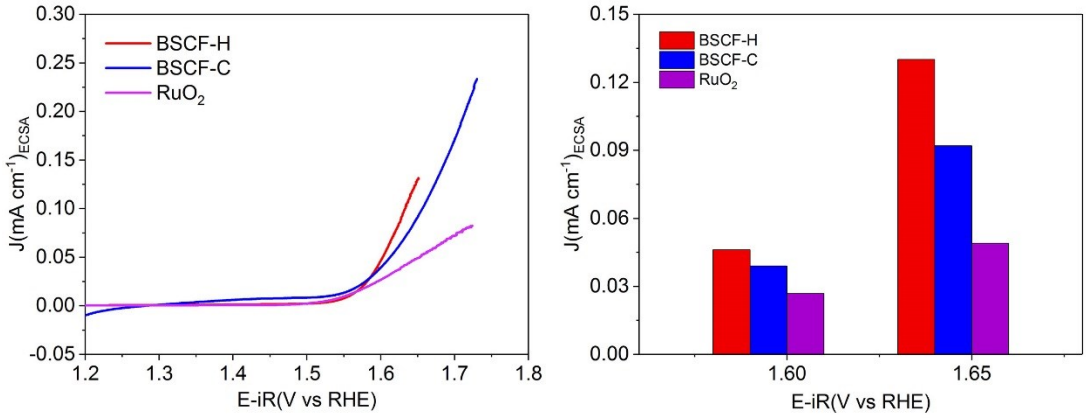

Fig. S5. (a) The OER specific activity of the BSCF-H, BSCF-C, and commercial RuO_2 catalysts. (b) Specific activity of the BSCF-H, BSCF-C, and commercial RuO_2 catalysts at potential of 1.60 and 1.65 V, respectively.

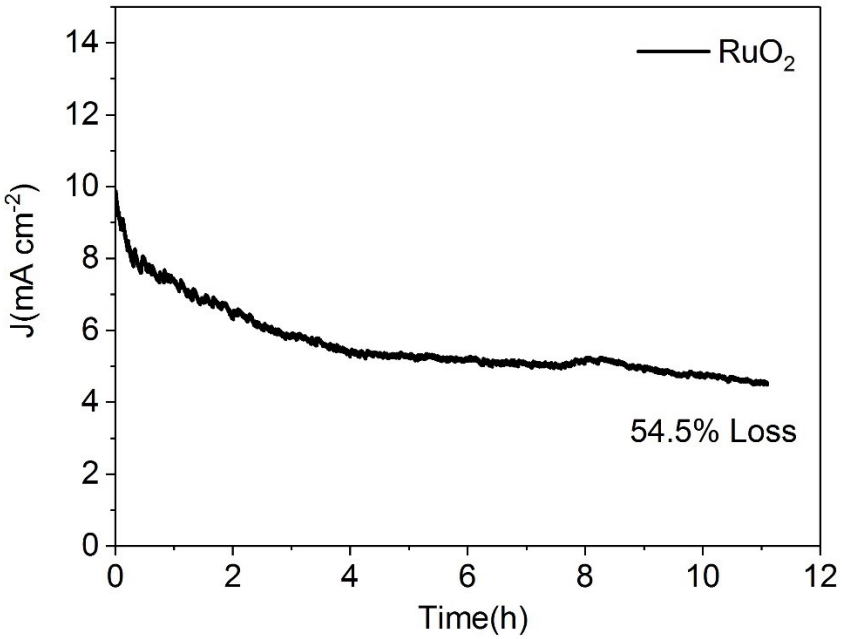

Fig. S6. Chronoamperometric responses of RuO_2 at constant potentials of 1.60 V ensure an initial current density of 10 mA cm^{-2}.

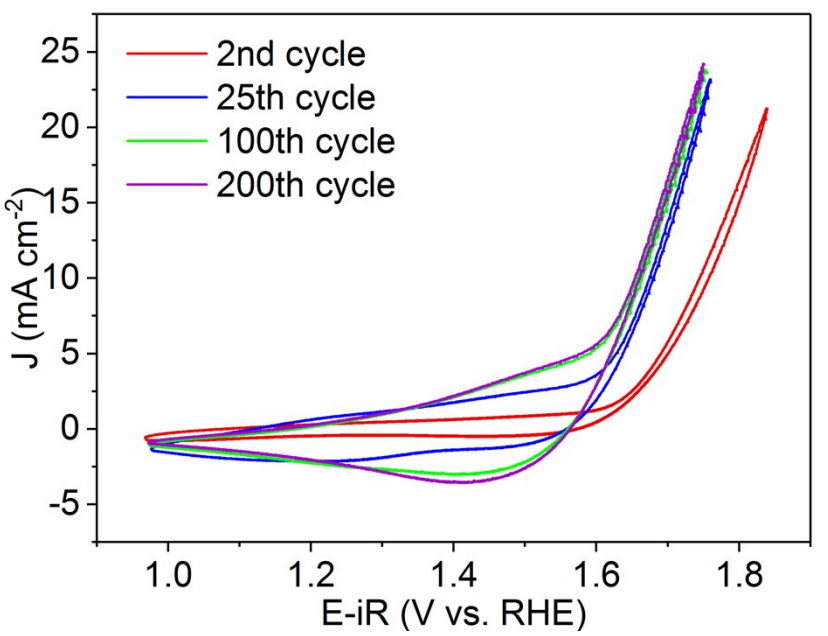

Fig. S7. Cyclic voltammograms (10 mV s^{-1}) of BSCF-H showing 2nd, 25th, 100th and 200th cycles.

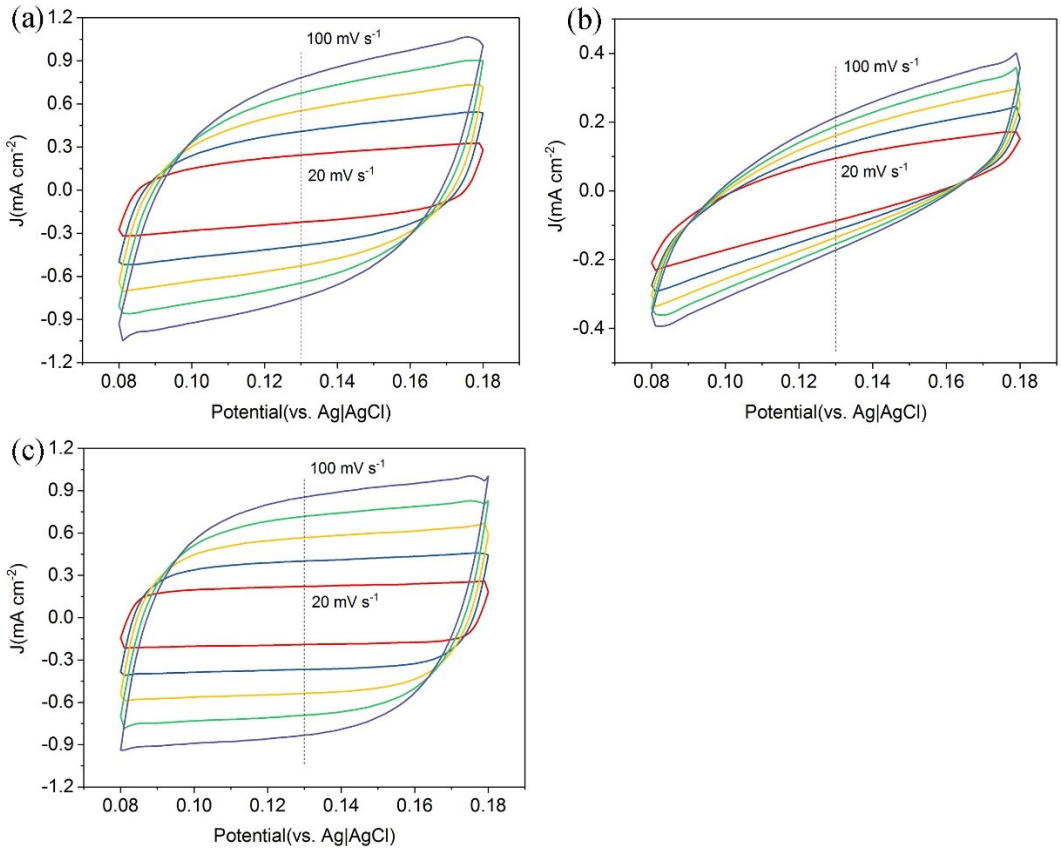

Fig. S8. CV measurements in a non-faradic current region (0.08-0.18 V vs. RHE, no iR-corrected) at scan rates of 20, 40, 60, 80 and 100 mV s^{-1} of (a) BSCF-H, (b) BSCF-C and (c) RuO_2 catalysts in 0.1 M KOH.

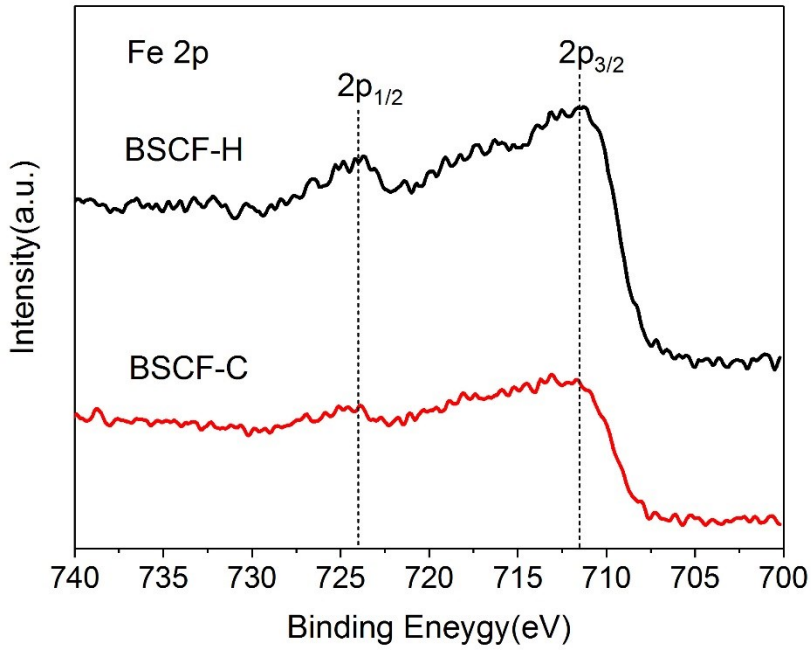

Fig. S9. XPS spectra of Fe 2p in the BSCF-H and BSCF-C.

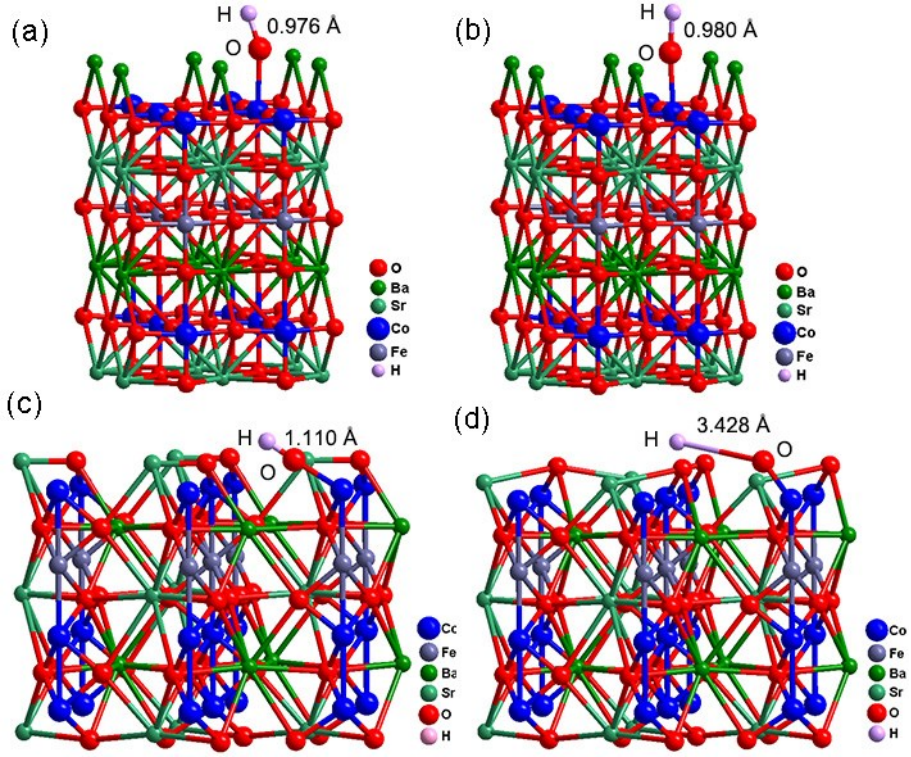

Fig. S10. (a) The initial HO and the optimized HO adsorption on the (001) surface of BSCF-C, (c) The initial HO adsorption and the optimized HO adsorption on the (001) surface of BSCF-H.

Table S1. Actual compositions of BSCF-H and BSCF-C powders by ICP-AES.

Samples	The concentrations of metal ions (μg/mL)				ICP-MS composition
	Ba	Sr	Co	Fe	
BSCF-H	35.34	18.82	19.56	4.589	Ba0.5Sr0.5Co0.8Fe0.2O3
BSCF-C	39.09	19.85	22.26	5.069	Ba0.5Sr0.5Co0.8Fe0.2O3

Table S2. Summary of OER activities of BSCF-H and some reported state-of-the-art perovskite catalysts based on transition metal. All catalysts supported on glass carbon electrode in 0.1 M KOH solution.

Catalysts	Tafel slope (mV dec-1)	Loading (mg cm^{-2})	η_{10} at 10 mA cm^{-2} (V)	References
$SrNb_{0.1}Co_{0.7}Fe_{0.2}O_{3-\delta}$ nanorod	61	0.232	≈0.39	*Adv. Energy Mater*. **2017**, *7*, 1602122
$PrBa_{0.5}Sr_{0.5}Co_{1.5}Fe_{0.5}O_{5+\delta}$ nanofiber	55	0.25	≈0.358	*Nat. Commun*, **2017**, 8, 14586
$La_{0.5}Sr_{1.5}Ni_{1-x}Fe_xO_{4\pm\delta}$	44	0.0153	≈0.36	*Nat. Commun*.，**2018**，9，3150
$SrCo_{0.95}P_{0.05}O_{3-\delta}$ (SCP)	84	0.232	≈0.48	*Adv. Funct. Mater.* **2016**, *26*, 5862–5872
$LaNiO_3$ Nanorods	N.A.	0.408	≈0.572	*ACS Appl. Mater. Interfaces* **2017**, 9, 24634-24648
$Pr_{0.5}Ba_{0.3}Ca_{0.2}CoO_{3-\delta}$	73	0.39	≈0.44	*Chem. Commun.*, **2017**, 53, 5132-5135
$Bi_{0.1}(Ba_{0.5}Sr_{0.5})_{0.9}Co_{0.8}Fe_{0.2}O_{3-\delta}$	74	0.2266	≈0.441	*Sci. Rep*. **2019**, 9, 4210
P-$Bi_{0.1}(Ba_{0.5}Sr_{0.5})_{0.9}Co_{0.8}Fe_{0.2}O_{3-\delta}$[a]	68	0.2266	≈0.37	*Sci. Rep.* **2019**, 9, 4210
La_2NiMnO_6-1	58	N.A.	≈0.37	*J. Am. Chem. Soc.* **2018**, 140, 11165-11169
SNCF-BM[b]	90	0.232	≈0.42	*Angew. Chem. Int. Ed.* **2015**,54, 3897-3901

$Ba_{0.5}Sr_{0.5}Co_{0.8}Fe_{0.2}O_{3-\delta}$	94	0.232	≈0.51	*Angew. Chem. Int. Ed.* **2015**,54, 3897-3901
BSCF-600[c]	63	0.232	≈0.36	*J. Mater. Sci. Technol.* **2019**, 35, 1184–1191
Cubic $Ba_{0.5}Sr_{0.5}Co_{0.8}Fe_{0.2}O_{3-\delta}$ (BSCF-C, 900℃)	118	0.25	≈0.47	This work
Hexagonal $Ba_{0.5}Sr_{0.5}Co_{0.8}Fe_{0.2}O_{3-\delta}$ (BSCF-H)	61	0.25	≈0.36	This work

[a]: BSCF-BM = ball-milling $Ba_{0.5}Sr_{0.5}Co_{0.8}Fe_{0.2}O_{3-\delta}$

[b]: P-$Bi_{0.1}(Ba_{0.5}Sr_{0.5})_{0.9}Co_{0.8}Fe_{0.2}O_{3-\delta}$ = plasma engraved $Bi_{0.1}(Ba_{0.5}Sr_{0.5})_{0.9}Co_{0.8}Fe_{0.2}O_{3-\delta}$

[c]: BSCF-600 = $Ba_{0.5}Sr_{0.5}Co_{0.8}Fe_{0.2}O_{3-\delta}$ by CO_2 thermal treatment

Table S3. The element concentration of Ba and Sr in the 0.1 M KOH solution after 10 h chronoamperometry test.

Sample	Ba element concentration(μg/L)	Sr element concentration(μg/L)
Reference (0.1 M KOH)	ND	ND
BSCF-C (0.1 M KOH)	24.44	236.5
BSCF-H (0.1 M KOH)	146.1	1254

ND = not detected

Table S4. The impedance parameters of the various catalysts performed in the present work.

catalysts	Rs (Ω)	Rct (Ω)
BSCF-H	37.29	19.52
BSCF-C	34.98	103.80
RuO_2	38.01	35.97

Table S5. O 1s XPS peak deconvolution results.

Electrocatalysts	lattice O^{2-}	O_2^{2-} /O^-	OH- or O_2	H_2O or CO_3^{2-}
BSCF-H	3.46%	32.93%	58.22%	5.39%
BSCF-C	11.17%	17.93%	64.18%	6.72%

References

1. M. D. Segall, P. J. D. Lindan, M. J. Probert, C. J. Pickard, P. J. Hasnip, S. J. Clark and M. C. Payne, First-principles simulation: ideas, illustrations and the CASTEP code, *J. Phys. Condens. Matter*, 2002, **14**, 2717-2744.
2. W. Xu, N. Apodaca, H. Wang, L. Yan, G. Chen, M. Zhou, D. Ding, P. Choudhury and H. Luo, A-site Excessive $(La_{0.8}Sr_{0.2})_{1+x}MnO_3$ Perovskite Oxides for Bifunctional Oxygen Catalyst in Alkaline Media, *Acs Catalysis*, 2019, **9**, 5074-5083.